

## Slow Internal Protein Dynamics from Water $^1\text{H}$ Magnetic Relaxation Dispersion

Erik P. Sunde and Bertil Halle\*

*Biophysical Chemistry, Center for Molecular Protein Science, Lund University, SE-22100 Lund, Sweden*

Received September 24, 2009; E-mail: bertil.halle@bpc.lu.se

Structural flexibility is essential to protein function, but the full range of internal dynamics has not yet been explored. Solution NMR relaxation methods routinely probe motions faster than  $\sim 10$  ns or slower than  $\sim 10$   $\mu\text{s}$ .<sup>1</sup> Residual dipolar couplings from weakly aligned proteins indicate fluctuations in the  $10^{-8}$ – $10^{-5}$  s window<sup>2</sup> but do not provide the associated correlation times. To study internal protein dynamics in this relatively inaccessible time window by NMR relaxation, isotropic averaging of spin couplings by protein tumbling must be prevented. This is accomplished by direct protein–protein contacts in microcrystals, studied by solid-state  $^{13}\text{C}$  or  $^{15}\text{N}$  relaxation,<sup>3</sup> or by covalent cross-links between fully hydrated proteins, studied by water  $^1\text{H}$ ,  $^2\text{H}$ , or  $^{17}\text{O}$  magnetic relaxation dispersion (MRD).<sup>4,5</sup>

In MRD studies of immobilized proteins, information about protein dynamics is conveyed to the observed bulk water resonance via internal water molecules and, for  $^1\text{H}$  and  $^2\text{H}$ , also via labile OH and NH hydrogens. If they exchange with bulk water on the relaxation time scale, these intermediary species probe protein dynamics in two ways. While residing on the protein, the intermediary species is dynamically coupled to the protein and thus reports on protein motions on time scales shorter than the residence time. Exchange plays the same role for an immobile protein as tumbling does for a free protein: it eliminates the effect of slower internal motions *and* induces relaxation by randomizing the orientation of the residual spin–lattice coupling tensor. For internal waters,<sup>5</sup> such exchange-mediated orientational randomization (EMOR) provides access to intermittent protein fluctuations involving highly excited conformational states. For exposed labile hydrogens, exchange is rate-limited by the chemical step so the residence time yields a protection factor but no information about protein dynamics.

The EMOR mechanism accounts quantitatively for water  $^1\text{H}$  and  $^2\text{H}$  MRD data from polysaccharide and polypeptide gels.<sup>6,7</sup> These gels are built from compact double or triple helices, and internal motions are not evident in the MRD data, except via intermittent fluctuations that control internal-water exchange. Globular proteins are more flexible, and slow side-chain motions have been detected by  $^2\text{H}$  MRD.<sup>5</sup> Whereas  $^2\text{H}$  relaxes by a single-spin electric-quadrupole mechanism, magnetic dipole–dipole couplings induce cross-relaxation between intermediary protons and nearby protein protons, potentially making  $^1\text{H}$  MRD a more sensitive probe of internal dynamics. To explore this possibility, we present here  $^1\text{H}$  MRD data from mammalian ubiquitin (mUb), immobilized by glutaraldehyde (GA) cross-linking of lysine side chains.<sup>8</sup> There is currently no consensus on the mechanism of water  $^1\text{H}$  relaxation in systems containing immobilized biomolecules, including biological tissue. Our second objective here is to resolve this issue by comparing  $^1\text{H}$  MRD data from deuterated and protonated forms of ubiquitin.

We analyzed the  $^1\text{H}$  MRD data with the most general version of the EMOR approach,<sup>7b</sup> with the 1.8 Å resolution crystal structure (1UBQ)<sup>9</sup> of mUb as input, as well as with an alternative, essentially

phenomenological, approach.<sup>4</sup> The latter approach rests on two major assumptions. First, a coarse-grained two-phase (2P) description<sup>10</sup> is used, based on the assumption that coherent spin diffusion and/or cross-relaxation is so fast that the  $^1\text{H}$  magnetization of the entire protein can be characterized by a single longitudinal relaxation rate  $R_{1\text{P}}(\omega_0)$ . The observed  $R_1$  is identified with the rate of the slowly decaying magnetization component in the 2P model,<sup>10</sup>

$$R_1 = (R_{1\text{P}} + R_{1\text{W}} + k)/2 - \{[R_{1\text{P}} - R_{1\text{W}} + (f_{\text{W}} - f_{\text{P}})k]^2/4 + f_{\text{P}}f_{\text{W}}k^2\}^{1/2} \quad (1)$$

where  $f_{\text{P}} = 1 - f_{\text{W}}$  is the fraction of protons that belong to the protein. The relaxation rate,  $R_{1\text{W}}$ , of the water phase and the protein–water magnetization exchange rate constant,  $k$ , are both taken to be frequency-independent.<sup>4</sup>

The alternative model further assumes that protein  $^1\text{H}$  relaxation is induced by small-amplitude collective vibration modes (“fractons”) in a direct mechanism akin to spin-phonon coupling in crystalline solids.<sup>11</sup> In this spin-fracton (SF) model,<sup>4</sup> the internal-motion time scale is set by a spectral dimension,  $d_{\text{S}}$ , that governs the low-frequency scaling of the vibrational density of states,  $\sigma(\omega) \propto \omega^{d_{\text{S}} - 1}$ , and one obtains<sup>4</sup>

$$R_{1\text{P}}(\omega_0) = 3\pi M_2 d_{\text{S}} \frac{k_{\text{B}}T}{\hbar} \Omega^{b-2} \left[ \frac{1}{\omega_0^b} + \frac{1}{(2\omega_0)^b} \right] \quad (2)$$

Here,  $M_2$  is the average  $^1\text{H}$  second moment of the protein,  $b = 3 - d_{\text{S}}(1 + 2/d_{\text{f}})$ ,  $d_{\text{f}}$  is the fractal dimension of the proton distribution, and  $\Omega$  is a high-frequency mode cutoff.<sup>12</sup>

Although the 2PSF and EMOR models differ in physical content, they can both provide adequate fits to  $^1\text{H}$  MRD data. However, the two models make very different predictions about the effect of H→D substitution in the protein, and they can therefore be discriminated by comparing the  $^1\text{H}$  MRD profiles from partially deuterated (D-mUb) and fully protonated (H-mUb) ubiquitin. Analysis of  $^1\text{H}$  NMR spectra (Figure S1) from the two proteins shows that 83% of the 485 nonexchangeable hydrogen sites are deuterated in D-mUb. Because the protein is dissolved in  $\text{H}_2\text{O}$ , essentially all OH and NH sites carry protons, but the hydrophobic core is extensively deuterated (Figure 1). The experimental results show that protein deuteration reduces  $R_1$  by merely 20% (Figure 2).

In the 2PSF model, deuteration affects  $R_1$  mainly via the reduction of  $f_{\text{P}}$  (by a factor 2.8) and  $M_2$  (by a factor 3.1). But these global variables only capture a part of the isotope effect. The fracton modes are thought to propagate mainly along the backbone.<sup>4</sup> The effective  $M_2$  should then be dominated by the mostly  $\beta$ -strand backbone of mUb, where  $\text{H}^\alpha$  deuteration increases the nearest-neighbor H–H separation by a factor of 2, thereby reducing the effective  $M_2$  by an order of magnitude.

As a result of these H→D substitution effects, the 2PSF model predicts at least an order-of-magnitude reduction of  $R_1$  at low

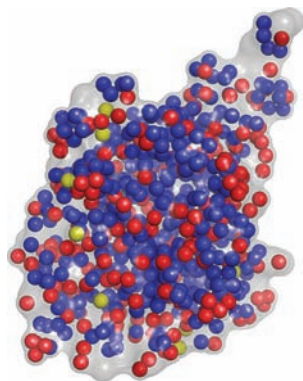


**Figure 1.** Crystal structure of mUb,<sup>9</sup> showing the D (blue), OH (yellow), and other H atoms (red) in the studied D-mUb variant.

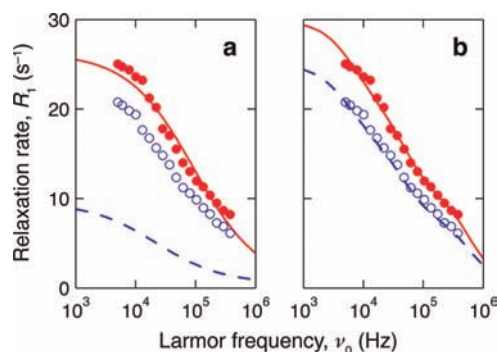


**Figure 2.** Water <sup>1</sup>H MRD profiles from immobilized H-mUb (●) and D-mUb (○) at pH 5.3, 20 °C, and a H<sub>2</sub>O/mUb mole ratio of 4000. The dashed curves are predictions of the (a) 2PSF and (b) EMOR models for the D-mUb profile, based on fits (solid curves) to the H-mUb data. The 2PSF prediction for D-mUb is an upper bound.

frequencies, whereas a mere 20% reduction is observed. We therefore conclude that the SF mechanism can account for at most a small fraction of the observed  $R_1$ . To illustrate the isotope effects on  $R_1$  that enter via  $f_P$  and the average  $M_2$ , we determined  $b = 0.78$  and  $k = 364 \text{ s}^{-1}$  from a fit<sup>12</sup> of eqs 1 and 2 to the H-mUb data (Figure 2a, solid curve). We then used these parameter values and the known deuteration pattern to predict the MRD profile for D-mUb (Figure 2a, dashed curve). Even though this simple analysis underestimates the isotope effect on  $R_{1P}$  (see above), the H→D substitution effect on  $R_1$  predicted by the 2PSF model is a factor of 3–4 larger than the observed effect (Figure 2a).

We now ask if the EMOR model can account for the isotope effect. With a residence time of 20 ns and an <sup>17</sup>O order parameter of 0.6,<sup>5</sup> the single internal water molecule in mUb makes a negligible ( $<0.2 \text{ s}^{-1}$ ) contribution to  $R_1$ . At pH 5.3, mUb contains 0.8 COOH protons and their contribution is also negligible ( $<0.1 \text{ s}^{-1}$ ). We thus conclude that the 11 hydroxyl protons (most of which are fully solvent-exposed; see Figure 1) are responsible for the <sup>1</sup>H dispersion. In H<sub>2</sub>O solvent at pH 5.3, their residence times should be on the order of  $10^{-2} \text{ s}$ , but additional proton exchange catalysis by PIPES buffer and excess GA reaction products evidently reduce this to  $\sim 10^{-4} \text{ s}$ .

As for the 2PSF model, we determined EMOR parameters from a fit<sup>13</sup> to the H-mUb profile (Figure 2b, solid curve) and then used these three parameters and the known deuteration pattern to predict the D-mUb profile (Figure 2b, dashed curve). The agreement between predicted and measured  $R_1$  indicates that the EMOR model captures the essential features of the relaxation mechanism. With residence times on the order of  $10^{-4} \text{ s}$ , the EMOR dispersion is close to the adiabatic limit where the dispersion frequency is given by the inverse dipole coupling.<sup>7</sup> For relaxation induced by a pure EMOR mechanism, with OH protons exchanging from a rigid protein, we thus expect a nearly Lorentzian dispersion centered at  $\sim 20 \text{ kHz}$ . The observation of a more extended MRD profile indicates internal motions of substantial amplitude on a  $\mu\text{s}$  time scale. For the fit in Figure 2b, a model-free spectral density function was used, yielding a correlation time  $\tau_{\text{int}} = 2.7 \mu\text{s}$  and an order parameter  $S_{\text{int}} = 0.47$ .<sup>14</sup> Interestingly,  $\mu\text{s}$  side-chain motions in mUb have also been inferred from residual dipolar couplings.<sup>2b</sup>

In summary, MRD data on deuterated mUb support the EMOR model for water <sup>1</sup>H relaxation in immobilized proteins but are incompatible with the 2PSF model. The present analysis also demonstrates that <sup>1</sup>H MRD provides information about side-chain dynamics in the  $10^{-8}$ – $10^{-5} \text{ s}$  time window.

**Acknowledgment.** This work was supported by the Swedish Research Council and the Knut and Alice Wallenberg foundation.

**Supporting Information Available:** Figure S1, Table S1, experimental methods, and data analysis protocol. This material is available free of charge via the Internet at <http://pubs.acs.org>.

## References

- (1) (a) Palmer, A. G. *Chem. Rev.* **2004**, *104*, 3623–3640. (b) Igumenova, T. I.; Frederick, K. K.; Wand, A. J. *Chem. Rev.* **2006**, *106*, 1672–1699. (c) Mittermaier, A.; Kay, L. E. *Science* **2006**, *312*, 224–228.
- (2) (a) Salmon, L.; et al. *Angew. Chem., Int. Ed.* **2009**, *48*, 4154–4157. (b) Farès, C.; Lakomek, N.-A.; Walter, K. F. A.; Frank, B. T. C.; Meiler, J.; Becker, S.; Griesinger, C. *J. Biomol. NMR* **2009**, *45*, 23–44.
- (3) (a) Giraud, N.; Blackledge, M.; Goldman, M.; Böckmann, A.; Lesage, A.; Penin, F.; Emsley, L. *J. Am. Chem. Soc.* **2005**, *127*, 18190–18201. (b) Agarwal, V.; Xue, Y.; Reif, B.; Skrynnikov, N. R. *J. Am. Chem. Soc.* **2008**, *130*, 16611–16621.
- (4) (a) Korb, J.-P.; Bryant, R. G. *J. Chem. Phys.* **2001**, *115*, 10964–10974. (b) Korb, J.-P.; Bryant, R. G. *Magn. Reson. Med.* **2002**, *48*, 21–26. (c) Korb, J.-P.; Bryant, R. G. *Biophys. J.* **2005**, *89*, 2685–2692.
- (5) Persson, E.; Halle, B. *J. Am. Chem. Soc.* **2008**, *130*, 1774–1787.
- (6) (a) Vaca Chávez, F.; Persson, E.; Halle, B. *J. Am. Chem. Soc.* **2006**, *128*, 4902–4910. (b) Vaca Chávez, F.; Hellstrand, E.; Halle, B. *J. Phys. Chem. B* **2006**, *110*, 21551–21559.
- (7) (a) Vaca Chávez, F.; Halle, B. *Magn. Reson. Med.* **2006**, *56*, 73–81. (b) Halle, B. *Magn. Reson. Med.* **2006**, *56*, 60–72.
- (8) Wine, Y.; Cohen-Hadar, N.; Freeman, A.; Frolow, F. *Biotechnol. Bioeng.* **2007**, *98*, 711–718.
- (9) Vijay-Kumar, S.; Bugg, C. E.; Cook, W. J. *J. Mol. Biol.* **1987**, *194*, 531–544.
- (10) (a) Zimmerman, J. R.; Brittin, W. E. *J. Phys. Chem.* **1957**, *61*, 1328–1333. (b) Koenig, S. H.; Brown, R. D. *Magn. Reson. Med.* **1993**, *30*, 685–695.
- (11) Abragam, A. *The Principles of Nuclear Magnetism*; Clarendon Press: Oxford, 1961.
- (12) For the fit, we used  $d_f = 2.5$  and  $\Omega = 1560 \text{ cm}^{-1}$  (corresponding to the amide-II band), as proposed,<sup>4</sup> and  $M_2 = 7.4 \times 10^9 \text{ s}^{-2}$ , based on the crystal structure 1UBQ with allowance for motional averaging.
- (13) For the EMOR analysis, the full  $610 \times 610$  relaxation matrix was used.
- (14) Internal motions were assigned to all dipole couplings with labile protons. Restricted rigid-body rotation of the entire protein in the gel network is expected to occur on the ns time scale and, in any case, does not agree well with the data. From  $R_1$  data above 1 MHz, we infer internal motions also on shorter time scales.

JA908144Y